Title

Computing trisections of 4-manifolds

Journal

Proceedings of the National Academy of Sciences of the United States of America, 115(43)

ISSN

0027-8424

Authors

Bell, Mark
Hass, Joel
Rubinstein, Joachim Hyam
et al.

Publication Date

2018-10-23

DOI

10.1073/pnas.1717173115

Peer reviewed

SPECIAL FEATURE

Computing trisections of 4-manifolds

Mark Bell[a], Joel Hass[b,1], Joachim Hyam Rubinstein[c], and Stephan Tillmann[d]

[a]Department of Mathematics, University of Illinois, Urbana, IL 61801; [b]Department of Mathematics, University of California, Davis, CA 95616; [c]School of Mathematics and Statistics, The University of Melbourne, Melbourne, VIC 3010, Australia; and [d]School of Mathematics and Statistics, The University of Sydney, Sydney, NSW 2006, Australia

Edited by David Gabai, Princeton University, Princeton, NJ, and approved July 9, 2018 (received for review October 23, 2017)

We describe an algorithm to compute trisections of orientable four-manifolds using arbitrary triangulations as input. This results in explicit complexity bounds for the trisection genus of a 4-manifold in terms of the number of pentachora (4-simplices) in a triangulation.

four-manifold | trisection | four-dimensional triangulations | topological algorithms | computational topology

A guiding principle in low-dimensional topology is to find practical algorithms to describe topological or geometric structures on manifolds and to compute invariants as well as to determine explicit complexity bounds for these algorithms. The steps in an algorithm reveal the structure of a manifold, and the complexity bounds relate the relative difficulty of a wide variety of problems. This paper is a first step toward a computational theory for understanding 4-manifolds via trisections. We use singular triangulations to give a description of a 4-manifold. These are well-established as a data structure for algorithmic 3-manifold theory (1–9) and have shown promise for analyzing manifolds in higher dimensions (10–12). Budney et al. (10) have developed a census of 4-manifold triangulations with up to six pentachora. This is a rich source of examples, and additional study or extension of this census requires algorithmic tools.

We develop a theory of colorings for 4-manifold triangulations, starting with a basic notion of *tricoloring* that encodes suitable maps to the 2-simplex and enhancing this to *c-tricoloring* with appropriate connectivity properties and *ts-tricoloring*, which completely encodes a trisection. This refines previous work of two of the authors (13).

1. Introduction

Gay and Kirby (14) introduced the concept of a *trisection* for arbitrary smooth, oriented, closed 4-manifolds. In dimensions less than or equal to four, there is a bijective correspondence between isotopy classes of smooth and piecewise linear structures (15, 16). All manifolds are assumed to be piecewise linear (PL) and orientable in this paper unless stated otherwise. Our definition and results apply to any compact smooth manifold by passing to its unique PL structure (17).

Definition 1 (trisection of closed manifold): Let M be a closed, orientable, connected PL 4-manifold. A *trisection* of M is a collection of three PL submanifolds $H_0, H_1, H_2 \subset M$, subject to the following four conditions.

1. Each H_i is PL homeomorphic to a standard PL four-dimensional 1–handlebody of genus g_i.
2. The handlebodies H_i have pairwise disjoint interiors, and $M = \bigcup_i H_i$.
3. The intersection $H_i \cap H_j$ of any two of the handlebodies is a three-dimensional 1–handlebody.
4. The common intersection $\Sigma = H_0 \cap H_1 \cap H_2$ of all three handlebodies is a closed, connected surface, the *central surface.*

The orientability of M implies that each of the handlebodies and the central surface in a trisection of M are orientable. The submanifolds $H_{ij} = H_i \cap H_j$ and Σ are referred to as the *trisection submanifolds*. In our illustrations, we use the colors blue, red, and green instead of zero, one, and two, and we will refer to $H_{\text{blue red}} = H_{br}$ as the *green* submanifold and so on.

The above definition is somewhat more general than the one originally given by Gay and Kirby (14) in that they ask for the trisection to be *balanced* in the sense that each handlebody H_i has the same genus. It was noted in ref. 13 that any unbalanced trisection can be stabilized to a balanced one. We also remark that the above definition and our methods naturally extend to nonorientable 4-manifolds, but here, we restrict ourselves to the setting of orientable manifolds following ref. 14. A representation of a trisection, dropping down two dimensions, is shown in Fig. 1. This representation completely encapsulates our approach. We wish to define maps from 4-manifolds to the 2-simplex such that the *dual cubical structure* of the 2-simplex pulls back to trisections of the 4-manifolds.

We use *singular triangulations* to give a concrete description of a 4-manifold M. To induce a trisection of M, we use maps from M to the standard 2-simplex Δ^2 that are induced by what we call *tricolorings*. The aim of this note is to describe an algorithm to compute a *trisection diagram* on the central surface given an arbitrary singular triangulation of M and to obtain complexity bounds on this description in terms of the size of the input triangulation. The definitions are motivated by the example given in the next section and illustrated in Fig. 2.

2. Example

Consider the moment map from the complex projective plane to the standard two-dimensional simplex $\mu\colon \mathbb{C}P^2 \to \Delta^2 \subset \mathbb{R}^3$ defined by

$$[\, z_0 : z_1 : z_2 \,] \mapsto \frac{1}{\sum |z_k|} \left(|z_0|, |z_1|, |z_2|\right).$$

The *dual spine* Π^2 in Δ^2 is the subcomplex of the first barycentric subdivision of Δ^2 spanned by the 0-skeleton of the first

Significance

Algorithms that decompose a manifold into simple pieces reveal the geometric and topological structure of the manifold, showing how complicated structures are constructed from simple building blocks. This note describes a way to algorithmically construct a trisection, which describes a four-dimensional manifold as a union of three four-dimensional 1-handlebodies. The complexity of the 4-manifold is captured in a collection of curves on a surface, which guide the gluing of the 1-handlebodies. The algorithm begins with a description of a manifold as a union of pentachora or four-dimensional simplices. It transforms this description into a trisection.

Author contributions: M.B., J.H., J.H.R., and S.T. performed research and wrote the paper.

The authors declare no conflict of interest.

This article is a PNAS Direct Submission.

[1]To whom correspondence should be addressed. Email: jhass@ucdavis.edu.

Published online October 22, 2018.

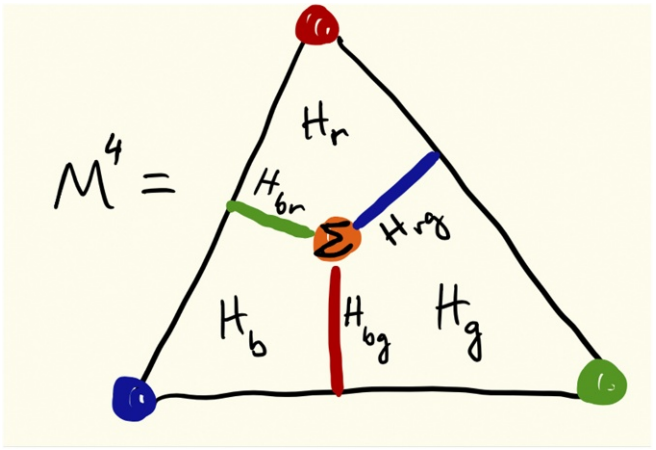

Fig. 1. Cartoon of a trisection.

barycentric subdivision minus the 0-skeleton of Δ^2. Decomposing along Π^2 gives Δ^2 a natural *dual cubical structure* with three 2-cubes, and the lower-dimensional cubes that we will focus on are the intersections of nonempty collections of these top-dimensional cubes, consisting of three *interior 1-cubes* and one *interior 0-cube*. The cubical structure is indicated in Fig. 1, where the interior cubes are labeled with the trisection submanifolds.

Under the moment map, the 2-cubes pull back to 4-balls

$$\{[z_0 : z_1 : z_2] \mid z_i = 1, |z_j| \leq 1, |z_k| \leq 1\};$$

the interior 1-cubes pull back to solid tori $S^1 \times D^2$ defined by

$$\{[z_0 : z_1 : z_2] \mid z_i = 1, |z_j| = 1, |z_k| \leq 1\};$$

and the interior 0-cube pulls back to a 2-torus $\Sigma = S^1 \times S^1$ defined by

$$\{[z_0 : z_1 : z_2] \mid z_0 = 1, |z_1| = 1, |z_2| = 1\}.$$

The central surface is thus a Heegaard surface for the 3-sphere boundary of each 4-ball. This shows that the cubical structure pulls back to a trisection with central surface a torus. This is shown schematically in Fig. 2.

Note that the midpoint of each edge of the 2-simplex pulls back to a circle defined by

$$\{[z_0 : z_1 : z_2] \mid z_i = 0, z_j = 1, |z_k| = 1\}.$$

This is the core circle of the corresponding solid torus. Each vertex of the 2-simplex Δ^2 pulls back to a singleton

$$\{[z_0 : z_1 : z_2] \mid z_i = 0, z_j = 0, z_k = 1\}.$$

There is more information in this picture. The central surface is the preimage of the barycenter of Δ^2, and each solid torus is the preimage of the line segment joining this to the barycenter of a facet of Δ^2. This identifies the boundary curves of the three meridian discs. Any two of these three curves give a Heegaard diagram for a 3-sphere, and the union of all three curves is called a *trisection diagram* by Gay and Kirby (14).

3. Constructing Trisection Diagrams

In this section, we define three notions of a tricoloring and describe an algorithm to compute trisections and trisection diagrams based on these colorings. We will see that these colorings are readily constructed on triangulated 4-manifolds.

Singular Triangulations. Let $\widetilde{\Delta}$ be a finite union of pairwise disjoint, oriented Euclidean 4-simplices with the standard simplicial structure. We call a 4-simplex a *pentachoron*. Every k-simplex τ in $\widetilde{\Delta}$ is contained in a unique pentachoron σ_τ. A 3-simplex in $\widetilde{\Delta}$ is called a *facet*, and a 0-simplex is a *vertex*.

Let Φ be a family of orientation-reversing affine isomorphisms pairing the facets in $\widetilde{\Delta}$, with the properties that $\varphi \in \Phi$ if and only if $\varphi^{-1} \in \Phi$, and every facet is the domain of a unique element of Φ. The elements of Φ are called *face pairings*.

We denote $\mathcal{T} = (\widetilde{\Delta}, \Phi)$. Any operation O of simplicial topology that is performed on $\widetilde{\Delta}$ (such as barycentric subdivision, regular neighborhoods, and so on) is said to be an operation on $\mathcal{T}$ as long as it respects the face pairings. The set of all face pairings Φ determines a natural equivalence relation on the set of all k-simplices in $\widetilde{\Delta}$, and we will call the equivalence classes the (*singular*) k-*simplices* of $\mathcal{T}$. This terminology is natural when passing to the quotient space $|\mathcal{T}| = \widetilde{\Delta}/\Phi$ with the quotient topology. The space $|\mathcal{T}|$ is a closed, orientable four-dimensional pseudomanifold, and the quotient map is denoted $p\colon \widetilde{\Delta} \to |\mathcal{T}|$. The set of nonmanifold points of $|\mathcal{T}|$, if any, is contained in the 1-skeleton [the work by Seifert and Threfall (18)].

A *singular triangulation* of a 4-manifold M is a PL homeomorphism $|\mathcal{T}| \to M$, where $|\mathcal{T}|$ is obtained as above. The triangulation is *simplicial* if $p\colon \widetilde{\Delta} \to |\mathcal{T}|$ is injective on each simplex. The triangulation is *PL* if, in addition, the link of every simplex is PL homeomorphic to a standard sphere: $\partial([0,1]^n)$.

Tricolorings. Let M be a closed, connected 4-manifold with (possibly singular) triangulation $|\mathcal{T}| \to M$. A partition $\{P_0, P_1, P_2\}$ of the set of all vertices of $\mathcal{T}$ is a *tricoloring* if every pentachoron meets two of the partition sets in two vertices and the remaining partition set in a single vertex. In this case, we also say that the triangulation is *tricolored*.

Denote the vertices of the standard 2-simplex Δ^2 by v_0, v_1, and v_2. A tricoloring determines a natural map $\mu\colon M \to \Delta^2$ by sending the vertices in P_k to v_k and extending this map linearly over each simplex. Note that the preimage of v_k is a graph Γ_k in the 1-skeleton spanned by the vertices in P_k.

As in the example of the complex projective plane, we would like to use μ to pull back the dual cubical structure of the simplex to a trisection of M. The preimages of the dual cubes have very simple combinatorics. The barycenter of Δ^2 pulls back to exactly one 2-cube in each pentachoron of M, and these glue together to form a surface Σ in M. This surface is the common boundary of each of three 3-manifolds obtained as preimages of an interior 1-cube (edge) of Δ^2. Each such 3-manifold is made up of cubes and triangular prisms as in Fig. 3. Each interior 1-cube c has a boundary of the union of the barycenter of Δ^2 and the barycenter b of an edge of Δ^2. Since the map $\mu\colon M \to \Delta^2$ is linear on each simplex, the preimage $\mu^{-1}(c)$ collapses to the preimage $\mu^{-1}(b)$. In particular, each 3-manifold has a spine made up of 1-cubes and 2-cubes. Recall that a compact subpolyhedron P in the interior of a manifold M is called a (PL) spine of M if M collapses to P. If P is a spine of M, then $M \setminus P$ is PL homeomorphic with $\partial M \times [0,1)$.

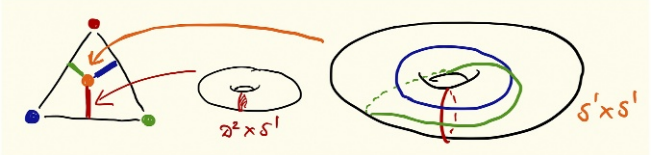

Fig. 2. Trisection diagram for $\mathbb{C}P^2$.

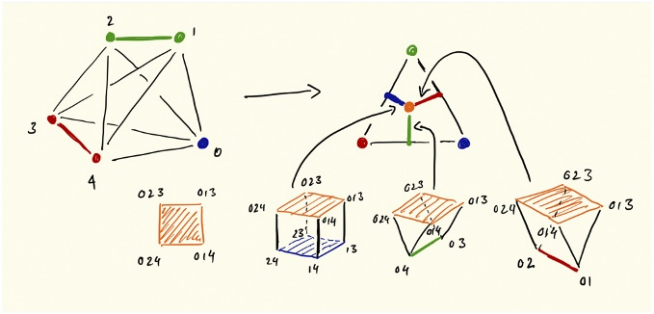

Fig. 3. Pieces of the trisection submanifolds. The vertices of the pieces are barycenters of faces and labeled with the corresponding vertex labels. The central surface meets the pentachoron in a square. Two of the three-dimensional trisection submanifolds meet the pentachoron in triangular prisms, and the third (corresponding to the singleton) meets it in a cube. Moreover, any two of these meet in the square of the central surface.

To see that the above construction gives a trisection, it suffices to show that

1. the graph Γ_k is connected for each k and
2. the preimage of an interior 1-cube of Δ^2 has a one-dimensional spine.

These conditions will be verified in the proof of the correctness of *Construction 3* below. The first condition ensures that the preimage of each 2-cube of Δ^2 is a connected, orientable four-dimensional 1-handlebody. In particular, it has connected orientable boundary. We claim that the second condition guarantees that the preimage under μ of each interior 1-cube of Δ^2 is a three-dimensional 1-handlebody; hence, it also has connected boundary. A priori, this preimage may be a union of three-dimensional 1-handlebodies. However, the boundary of the four-dimensional 1-handlebody is the union of such three-dimensional handlebodies, and each of them has connected boundary: hence, the claim. This also implies that the central surface is connected.

We say that a tricoloring is a *c-tricoloring* if Γ_k is connected for each k and that a c-tricoloring is a *ts-tricoloring* if the preimage of each interior 1-cube collapses onto a one-dimensional spine. In this case, the dual cubical structure of Δ^2 pulls back to a trisection of M.

For example, the standard 4-sphere S^4 can be realized as a doubled pentachoron, giving it a singular triangulation with two pentachora and five vertices, denoted $v_0, \dots, v_4$. Letting $P_0 = \{v_0, v_1\}$, $P_1 = \{v_2, v_3\}$, and $P_2 = \{v_4\}$ gives a ts-tricolored triangulation of S^4 with each of Γ_0 and Γ_1 being a 1–simplex and Γ_2 being a 0–simplex.

An examples of a c-tricoloring that is not a ts-tricoloring can be found in Section 6.

Existence of Tricolorings. In general, given an arbitrary triangulated 4-manifold M, one can always obtain a tricolored triangulation by passing to the first barycentric subdivision. This has a natural partition of the vertices into five sets B_i (the barycenters of the k-simplices for $0 \le k \le 4$). Any coarsening of this partition of the form $\{B_i \cup B_j, B_k \cup B_l, B_m\}$ now gives a tricoloring. For instance, the partition $\{B_0 \cup B_1, B_2 \cup B_3, B_4\}$ was used in ref. 13. While conceptually simple, this process multiplies the number of pentachora by a factor of 120. We now give an improved construction.

A *bistellar move*, also called a *Pachner move*, consists of replacing a set of pentachora that embed in a 5-simplex Ω by the complementary set of pentachora in Ω. This also generalizes to a singular triangulation by allowing identifications consistent with the replacement. These moves are called 1–5, 2–4, 3–3, 4–2, and 5–1 moves.

Construction 2. *Given an arbitrary triangulation of a closed 4-manifold M having n pentachora, there is a triangulation with $60n$ pentachora that admits a tricoloring with the property that two of the graphs Γ_k are connected and the third consists of isolated vertices.*

Proof: Let $|\mathcal{T}| \to M$ be a (possibly singular) triangulation of M. Each pentachoron σ in $\mathcal{T}$ has a natural subdivision into 60 pentachora, with a set of vertices consisting of its 0-simplices together with its barycenter and all barycenters of its 2-simplices and 3-simplices. This can be built by first applying a 1–5 bistellar move to σ. Each new pentachoron $\sigma' < \sigma$ has a unique 3-face that corresponds to a 3-simplex in σ. Perform a 1–4 move on this 3-simplex, and cone this to a triangulation of σ' consisting of four pentachora. Each of the resulting pentachora σ'' contains a unique 2-simplex that corresponds to a 2-simplex in σ. Perform a 1–3 move on this 2-simplex, and cone this to a triangulation of σ''.

For each pentachoron σ in the resulting triangulation, there is a flag $\sigma^1 < \sigma^2 < \sigma^3 < \sigma^4$ of simplices, such that the vertices of σ consist of the vertices of σ^1 and the barycenters of σ^2, σ^3, and σ^4. The tricoloring is now obtained by placing the vertices of σ^1 in the set P_0, the barycenter of σ^2 in the set P_1, and the barycenters of σ^3 and σ^4 in the set P_2. This gives a tricoloring with $60n$ pentachora.

The graphs Γ_0, Γ_2 are connected, because they are the 1-skeleton and dual 1-skeleton of the original triangulation. Furthermore, Γ_1 consists of isolated vertices, because each pentachoron has exactly one vertex in the set P_1. □

From Tricolorings to ts-Tricolorings. We now show that, given any tricolored triangulation of M, there is a simple procedure that transforms it into a ts-tricolored triangulation of M.

Construction 3. *Given a tricolored triangulation of the closed 4-manifold M with n pentachora, there is a ts-tricolored triangulation with $2n$ pentachora.*

Proof: In a tricolored triangulation, each pentachoron σ has a unique facet τ that meets only two of the partition sets. There is a unique pentachoron σ' meeting σ in τ, and the two together form a *double pentachoron* $\sigma \cup_\tau \sigma'$. The manifold M thus has a decomposition into double pentachora.* There are three types of double pentachora classified by the isolated vertices. Shown in Fig. 4 is a double pentachoron with vertices numbered one to four in τ (drawn in green and red in Fig. 4) and zero and five not in τ (drawn in blue in Fig. 4). The three colors correspond to the partition sets P_k, and vertices of the same color may be identified in M. Throughout this proof, we may without loss of generality refer to this labeled double pentachoron. The other two types arise by permuting the three colors.

We focus on one of the partition sets, P_k. The graph Γ_k meets a double pentachoron either in a single edge or in two isolated vertices. We perform a 2–4 move on each of the double pentachora meeting Γ_k in two isolated vertices. This gives a new triangulation $\mathcal{T}'$ and a new graph Γ'_k. Each pentachoron in $\mathcal{T}'$ meets Γ'_k in an edge, and hence, the graph Γ'_k is connected. To see that Γ'_k is connected, choose any two vertices in P_k contained in two pentachora of the triangulation. A path in the dual 1-skeleton between barycenters of these pentachora can be deformed into Γ'_k after the 2–4 moves, showing that this graph is indeed connected.

Notice that Γ'_k is obtained from Γ_k by adding one edge for each double pentachoron on which a 2–4 move was performed.

*To the knowledge of the authors, this elementary fact has not been observed previously.

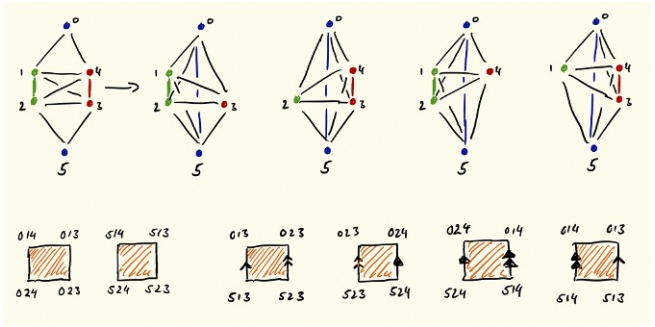

Fig. 4. Converting a double pentachoron to a quadrapentachoron. Also shown are the squares of the central submanifold—the move replaces two disjoint discs with an annulus, thus adding a handle to the central surface. The remaining figures are based on this; there are two other kinds of pentachoron corresponding to permutations of the colors.

In Fig. 4, vertices in P_k are drawn in blue. This does not affect any of the other monochromatic graphs. Since this can be done independently for each k (adding edges does not change the other graphs), this shows that, after doing all 2–4 moves, we have a c-tricoloring.

We claim that, in fact, we also have a ts-tricoloring after performing all 2–4 moves. This has to do with special properties of the degree four edges obtained in doing these moves. Let us introduce some additional terminology that will be useful. A 2–4 move performed on a double pentachoron gives a *quadrapentachoron*: that is, a collection of four pentachora meeting in a common 1-simplex contained in no other pentachora and with a particular coloring having two vertices of each color. This structure of the quadrapentachora is crucial to our constructions and proofs.

Let Q be a collection of four pentachora forming one of these quadrapentachora. The boundary of Q consists of eight tetrahedral, and M is tiled by disjoint collections of these quadrapentachora, meeting along common tetrahedral faces. After the collection of 2–4 moves, there are four steps.

1. The monochromatic subgraph of the 1-skeleton Γ_k is connected for each k.
2. $\Sigma \cap Q$ is an annulus formed from squares, one square in each of the four pentachora of Q. The boundary of this annulus consists of eight edges lying in eight boundary tetrahedra of Q, with eight vertices lying in eight boundary 2-simplices of Q. These combine to give a decomposition of Σ into annuli.
3. For each k and three-dimensional trisection submanifold H_{ij}, the intersection $H_{ij} \cap Q$ consists of one of two types of polyhedral structures.

The first polyhedral structure is a 3-ball $B \subset Q$ with a boundary that is tiled by eight square and four triangular faces. Four of the square faces form an annulus that is on Σ, and the others form a pair of discs lying in ∂Q. There is a collapse of B to a one-dimensional spine (an "H"), and on ∂Q, this collapse agrees with those defined on adjacent quadrapentachora. This follows from the facet pairings indicated in Fig. 5. For example, consider the red square that the red submanifold H_{bg} collapses to, which is shown in Fig. 5. This square has two edges, $(01, 51)$ and $(02, 52)$, that are in the interior of Q and thus, are not glued to any other red squares. Thus, the collapse to an H in Q matches with similar collapses in adjacent quadrapentachora.

The second polyhedral structure is a solid torus $T \cong S^1 \times D^2$ with a boundary that is tiled by 12 square faces. The boundary of T intersects ∂Q in eight of these square faces, two in each pentachoron of Q. This solid torus collapses to a curve consisting of four line segments, and on ∂Q, this collapse agrees with those on adjacent quadrapentachora (Fig. 6).

4. $X_k \cap Q$ is a 4-ball that collapses to $\Gamma'_k \cap Q$ and restricts on ∂Q to a collapse of $X_k \cap \partial Q$ that agrees with those on adjacent quadrapentachora.

This discussion shows that each pairwise intersection of four-dimensional handlebodies is indeed a three-dimensional handlebody, since it has a one-dimensional spine and hence, completes the proof. □

Combining *Constructions 2* and *3* gives *Theorem 4*.

Theorem 4. *Given an arbitrary triangulation of the closed orientable 4-manifold M having n pentachora, there is a triangulation with $120n$ pentachora that admits a ts-tricoloring.*

Constructing Trisection Diagrams. The *Proof of Construction 3* allows the construction of the compression discs of the three-dimensional handlebodies (and hence, the trisection diagram) from a ts-tricolored triangulation with a decomposition into quadrapentachora. The details will now be given.

The three-dimensional 1-handlebodies H_{ij} have a coarse decomposition into polyhedral balls and polyhedral solid tori, and they have a finer decomposition of each polyhedral ball into two 3-cubes and two triangular prisms and of each polyhedral torus into four triangular prisms. The initial spine for each H_{ij} consisted of a 2-cube in each polyhedral ball and of a circle consisting of four 1-cubes in each polyhedral solid torus. It was then shown that each 2-cube can be collapsed further to an H. To analyze the spine further, we use the natural simplicial subdivision of an H into five 1-simplices. Note that a square face of a polyhedral cube may glue to a square face of a polyhedral solid torus. We, therefore, also subdivide the 1-cubes in the polyhedral solid tori into two 1-simplices. This gives a consistent subdivision of the one-dimensional spine of H_{ij} (possibly with some redundancies that can be avoided in an efficient implementation).

We claim that, for each handlebody, a complete system of compression discs is constructed by adding canonical normal squares and normal triangles as shown in Fig. 7. In a polyhedral solid torus, there are two normal triangles in triangular prisms, which are dual to the two 1-simplices of the spine. In a polyhedral solid torus, there is one central square in each cube that is dual to the internal edge of the H, and each edge meeting a boundary vertex of the H has a corresponding dual square. To give well-defined discs in the polyhedral balls, we introduce three normal triangles in each triangular prism contained in it.

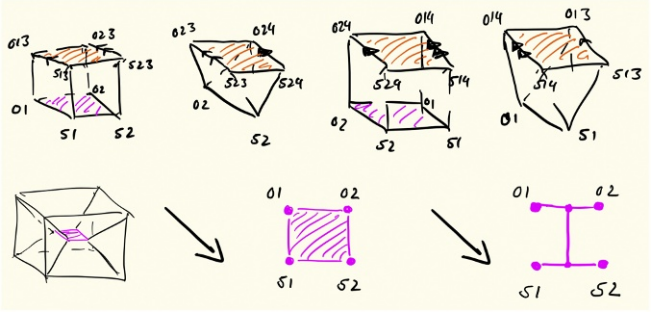

Fig. 5. Red submanifold (based on Fig. 4). Blocks that form pieces of trisection submanifolds. The vertices of the blocks are barycenters of faces of the triangulation labeled with the corresponding vertex labels. The picture for the green submanifold is analogous, with the notable difference that it meets the pentachora in cubes (prisms) that the red submanifold meets in prisms (cubes).

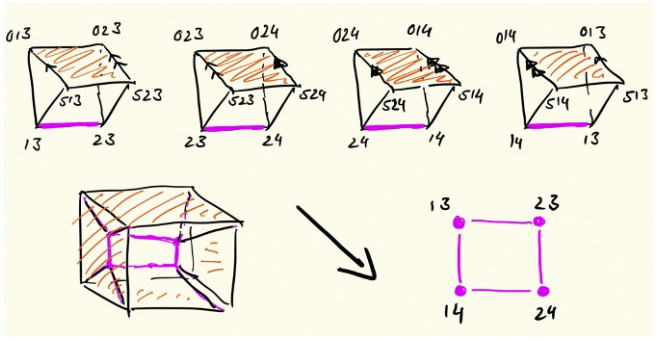

Fig. 6. Blue submanifold (based on Fig. 4). Blocks that form pieces of trisection submanifolds. The vertices of the blocks are barycenters of faces of the triangulation, labeled with the corresponding vertex labels.

The surface formed in each of the polyhedral structures is shown in Fig. 8. This directly shows that the surface meeting the internal edge of the H is a disc transverse to the spine and hence, a meridian disc.

For the remaining discs, we need to show that no branching occurs along the edges of the normal triangles and quadrilaterals. It follows from the labeling of barycenters that such an edge is in a 3-simplex in the triangulation and hence, meets at most two building blocks of the three-dimensional handlebody. Hence, the surface is properly embedded. The claim that each component is a disc now follows from the fact that each triangle meets a unique one-dimensional stratum of the spine in a vertex. Developing this surface normally to the spine around this central vertex can only give a disc.

To see the discs form a complete system (possibly with redundancies), note that each edge of the spine has a dual disc. The central surface Σ is decomposed along a graph into annuli. Each annulus is made up of four squares, giving the surface a natural singular Euclidean structure. Each such annulus is met in a single core curve and in two pairs of boundary parallel arcs by two of three sets of meridian curves. The remaining set meets the core curve transversely in eight essential arcs, one in each square. This is shown in Fig. 9.

One can make the placement of the discs in the blocks completely canonical as follows. Each 1-simplex that is in a subdivided 1-cube of the spine is oriented toward the midpoint of the 1-cube. One then marks the potential intersection points of normal discs with these 1-simplices as $\frac{1}{5}$ from the initial vertex for H_{12}, $\frac{2}{5}$ for H_{02}, and $\frac{3}{5}$ for H_{12}. Each internal edge of an H is oriented arbitrarily, and the potential intersection points are marked at $\frac{4}{10}$, $\frac{5}{10}$, and $\frac{6}{10}$, respectively. These placements can now be extended linearly over the cubes and prisms and give markings on the squares of the central surface. The resulting curves are hence transverse. After a clean-up step that removes parallel copies of curves, we obtain the desired trisection diagram.

4. Complexity Bounds

In this section, the aim is to give a bound for the genus of the central trisection surface in terms of the number of pentachora in a triangulation of a 4-manifold.

Theorem 5. *Suppose M is a closed orientable 4-manifold with a triangulation having a ts-tricoloring and n pentachora. Then, the genus of the central trisection surface is at most $n/2$.*

Proof: Every pentachoron contributes one quadrilateral to the central trisection surface Σ. Hence, Σ has a quadrangulation with n quadrilaterals, $2n$ edges, and at least one vertex. The Euler characteristic satisfies $\chi(\Sigma) \geq 1-n$, and this implies that $g(\Sigma) \leq (n+1)/2$. Since n is even, we have the claimed inequality. □

Corollary 6. *Suppose M is a closed orientable 4-manifold with an arbitrary triangulation with m pentachora. Then, there is a trisection with central surface having genus at most $60m$.*

Proof: This follows by combining the results of *Theorem 4* and *Theorem 5*. □

Since a surgery description of a 4-manifold M can be converted into a triangulation, this implies an upper bound for the genus of a trisection of M, with input of a Kirby diagram. It would be interesting to determine explicit complexity bounds on the trisection genus from different descriptions of 4-manifolds, such as Kirby diagrams.

Question 7. *Can one find general bounds that are asymptotically sharp for infinite families of examples?*

5. Moves Simplifying Tricolored Triangulations

Given a c-tricolored (ts-tricolored) triangulation, we give a criterion to obtain a *collapsed* triangulation that is also c-tricolored (ts-tricolored) but has only three vertices, one for each color. We also show that tricolored triangulations can be simplified with some bistellar moves while maintaining the coloring property.

Tricolored Triangulations with Few Vertices. An edge E of a triangulation $\mathcal{T}$ of a 4-manifold is contained in a bubble 2-sphere S if the following three conditions are satisfied.

1. There is an even collection of singular 2-simplices $F_1, F_2, \ldots, F_{2k}$ of $\mathcal{T}$, each containing the edge E.
2. For each i, the remaining edges of F_i can be labeled E_i^- and E_i^+, such that $E_i^+ = E_{i+1}^-$ and $E_{2k}^+ = E_1^-$.
3. If there is a tricoloring of the triangulation, then E is a monochromatic edge with ends on two different vertices.

We say that $\mathcal{T}^\star = (\widetilde{\Delta}^\star, \Phi^\star)$ is obtained from $\mathcal{T} = (\widetilde{\Delta}, \Phi)$ by *collapsing* the edge E if $\widetilde{\Delta}^\star$ consists of all pentachora in $\widetilde{\Delta}$ not containing the edge E, and the face pairings $\Phi^\star$ are obtained as follows. Each facet τ in $\widetilde{\Delta}^\star$ is the domain of a unique $\varphi_\tau \in \Phi$. If the codomain of φ_τ is also a facet in $\widetilde{\Delta}^\star$, then $\varphi_\tau \in \Phi^\star$. Otherwise, the codomain of φ_τ is a facet τ_1 of a pentachoron σ_1 containing E, and the collapse χ of σ_1 naturally identifies this with another facet τ_2 of σ_1. If the codomain of φ_{τ_2} is in $\widetilde{\Delta}^\star$, then we let $\varphi_{\tau_2} \circ \chi \circ \varphi_\tau \in \widetilde{\Delta}^\star$. Otherwise, this procedure propagates through a finite number of facets of collapsed pentachora until it terminates at a facet in $\widetilde{\Delta}^\star$. We note that, at this stage, no claim was made that $|\mathcal{T}^\star|$ is a manifold or PL equivalent with $|\mathcal{T}|$.

Theorem 8. *Suppose that $\mathcal{T}$ is a triangulation of a 4-manifold that admits a c-tricoloring (a ts-tricoloring) and that E is a monochromatic edge that is not contained in any bubble 2-sphere. If $\mathcal{T}^*$ is obtained by collapsing E, then $|\mathcal{T}^\star|$ is PL equivalent with $|\mathcal{T}|$, and $\mathcal{T}^*$ admits a c-tricoloring (a ts-tricoloring).*

Proof: Consider a monochromatic edge E joining two distinct vertices v, v' colored R without loss of generality. Each pentachoron σ containing E is the join of E and a triangular face Δ with vertices colored either BBG or BGG. The two tetrahedral facets τ, τ' of σ, with vertices being those of Δ and one of v, v',

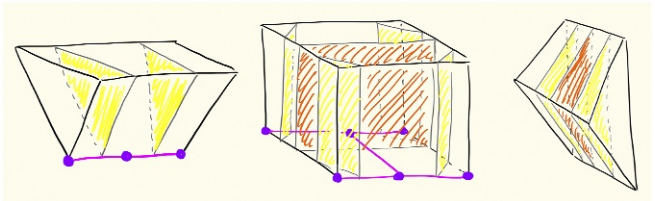

Fig. 7. Canonical triangles and squares in blocks. Shown from left to right are prism in torus, cube, and prism in ball.

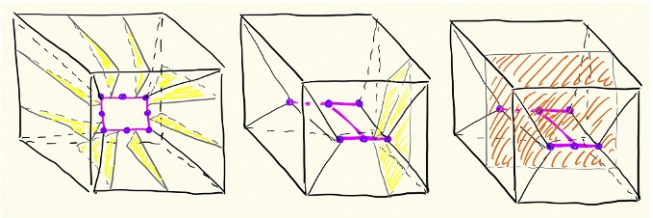

Fig. 8. Canonical triangles and squares in the polyhedral structures of the submanifolds: all discs in the torus structure (*Left*), one of the four discs parallel to vertical edges in the cube structure (*Center*), and the central discs in the cube structure (*Right*).

respectively, are identified when E is collapsed. Clearly, the collapse of E preserves the tricoloring, and each monochromatic subgraph is either unchanged or in the case of Γ_R, has the edge E collapsed to a vertex. Hence, the property of c-tricoloring is preserved. Moreover, the result of collapsing is a new manifold PL homeomorphic to the original one if the collapsing map is cell like (i.e., the inverse image of a point in the identification space after collapsing is either a point or a finite tree). This also implies that the property of ts-tricoloring is preserved. We claim that this map is cell like when E is not contained in any bubble 2-spheres.

The boundary of the collection of pentachora containing E is the suspension of the link S of E, where S is the set of triangular faces Δ as in the previous paragraph. Therefore, this boundary is the union of two cones over S, with cone points v, v'. Note that S is obtained from a 2-sphere with vertices all colored B, G and that any identifications of these cones must preserve the colorings.

Suppose a sequence $s_1, s_2, \dots s_k$ of pairs of edges joining two vertices of S either both to v or both to v' are identified. Assume also that, for s_i, s_{i+1} and s_k, s_1, one of the edges of each pair is collapsed to the same image. We can label the pairs of edges by $s_1 = \{E_1^+, E_2^-\}, \dots s_k = \{E_{2k}^+, E_1^-\}$. This produces a bubble 2-sphere and a loop in the inverse image of the points in these edges after collapsing. In fact, there is a singular foliation of the bubble 2-sphere by loops that are inverse images of points. The effect of collapsing is to map the bubble 2-sphere to an interval, which induces a surgery on the manifold. This shows why the absence of bubble 2-spheres is necessary and sufficient to ensure that collapsing E corresponds to a cell-like map. A general discussion of cell-like mappings in dimensions other than four is given in ref. 19.

We can construct the PL homeomorphism directly, since the cell-like collapsing map is of a simple type. We follow a method of J. W. Cannon, factoring the edge collapse into a sequence of small collapses using the skeleta of the triangulation.

Consider, for example, the inverse image of an edge E', where the inverse image of each interior point is a finite tree and the inverse image of one vertex is a single vertex and of the other vertex of E' is the edge E. The resulting 2-complex F is the union of a cone over the tree and the mapping cylinder of the map of the tree to the edge E as can be seen by decomposing over the inverse image of the midpoint of E'. Notice that F can be viewed as a tree of 2-simplices. F can be collapsed by homotoping leaf 2-simplices onto two of their boundary edges, one of which is E and the other of which is where the 2-simplex connects onto the rest of F, one 2-simplex at a time.

After collapsing all such inverse images of edges E', we can go on to collapse inverse images of 2-simplices etc. Note that each small collapse is then of a PL-embedded ball, namely a simplicial collapse of an embedded simplex. However, it is elementary to verify that collapsing such a ball gives a map that can be approximated by a PL homeomorphism. Therefore, this completes the proof. □

Suppose that $\mathcal{T}$ is a triangulation of a 4-manifold that admits a c-tricoloring (a ts-tricoloring). If, after each edge collapse, there are no bubble 2-spheres, then we can perform a series of edge collapses to obtain a new triangulation $\mathcal{T}^*$ that has a c-tricoloring (a ts-tricoloring) where each monochromatic graph has a single vertex and therefore, is a wedge of circles. In particular, $\mathcal{T}^*$ has precisely three vertices, one of each color. It is an interesting problem to determine whether such a series of triangulations without bubble 2-spheres can be found.

Simplifying Moves.

Theorem 9. *Suppose $\mathcal{T}$ is a triangulation of a 4-manifold that admits a tricoloring (a c-tricoloring).*

- *Suppose that $\mathcal{T}^*$ is obtained by performing a 5–1 move on $\mathcal{T}$. Then, $\mathcal{T}^*$ admits a tricoloring (a c-tricoloring).*
- *Suppose that $\mathcal{T}^*$ is obtained by performing a 4–2 move on $\mathcal{T}$. Then, $\mathcal{T}^*$ admits a tricoloring.*
- *Assume that $\mathcal{T}^*$ is obtained by performing a 3–3 move on $\mathcal{T}$ and that the three pentachora involved in the 3–3 move have six vertices with three sets of pairs of colors. Then, $\mathcal{T}^*$ admits a tricoloring.*

Proof: Recall that a bistellar move on a four-dimensional triangulation $\mathcal{T}$ consists of replacing a set of pentachora that embed in a 5-simplex Ω by the complementary set of pentachora in Ω. Now, Ω has six vertices and pentachora facets.

The facets coming from $\mathcal{T}$ are tricolored. Therefore, we see immediately in the cases of 5–1 and 4–2 moves that the vertices of Ω must be colored $RRBBGG$, because if there were three vertices of the same color, then the number of tricolored facets would be at most three. However, if there are two vertices of each color, then every facet is tricolored. Hence, in this case, every bistellar move associated with Ω yields a tricolored triangulation.

We now show that if $\mathcal{T}$ is c-tricolored, then so is $\mathcal{T}^*$. In the case of a 5–1 move, we can visualize this as replacing the cone on the facets of a pentachoron by the pentachoron. Suppose the facets

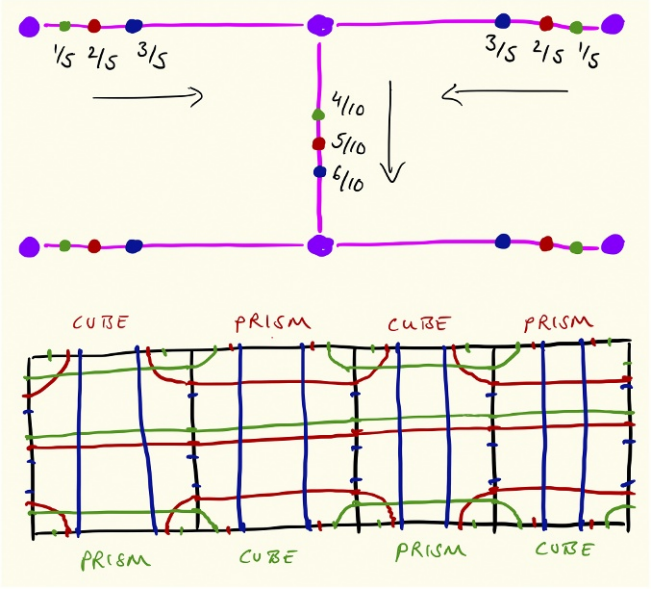

Fig. 9. The trisection diagram on a cubulated annulus of Σ: *Upper* shows the placement of the intersection points with the spine, and *Lower* shows the curves on the cubulated annulus consistent with Fig. 4. Also indicated is that, whenever the ball structure of the red submanifold meets a square of the central surface in a cube, then the ball structure of the green submanifold meets it in a prism and vice versa.

have vertices that are colored $RRBBG$ without loss of generality. Then, the central cone point is colored G. If the monochromatic subgraphs are connected before we do this bistellar move, it is easy to see they are still connected afterward, because only Γ_G changes by deleting the edge joining the two vertices colored G. This edge clearly has a leaf vertex of the tree Γ_G at the central cone point colored G. Therefore, this does not disconnect the subgraph.

Consider next a 4–2 move. Here, four pentachora share a common edge E. Each pentachoron can be viewed as the join of E and a triangular face $\sigma_i, 1 \leq i \leq 4$. The four triangles are faces of a tetrahedral facet Π, and the replacement can be viewed as two pentachora sharing a facet Π.

Suppose first that the two vertices of E have different colors, say BG without loss of generality. Then, Π has vertices with colors $RRBG$. As in the case of the 5–1 move, the monochromatic edges deleted under our 4–2 move end at leaf vertices at E and therefore, do not disconnect the monochromatic graphs.

Finally, assume that the vertices of E both have colors, say G. In this case, Π has vertices with colors $RRBB$. In particular, the monochromatic subgraphs Γ_R, Γ_B do not change, whereas Γ_G has E deleted. Therefore, this may disconnect Γ_G, and we may change a c-tricoloring into a tricoloring.

The case of a 3–3 move, where the three pentachora have six vertices colored $RRBBGG$, is similar to the case of a 4–2 move. In fact, such a move only gives a c-tricoloring from an initial c-tricoloring if the three pentachora share a triangular face with vertices colored RBG. □

6. Examples

After a tricoloring is found for a triangulation, one needs to check the two properties that the monochromatic graphs are connected and that the three-dimensional trisection submanifolds have one-dimensional spines. An example of a tricolorable triangulation, where the former property holds but the latter fails, is the triangulation of $S^1 \times S^3$ with isomorphism signature gLAAMQacbdcdefffcaTava4acavayaWaZa2a (20). This has six pentachora and three vertices. The three monochromatic graphs are circles, but the central surface consists of three pairwise disjoint 2-tori. Two ts-tricolorable triangulations with six pentachora and three vertices of this manifold were found by Jonathan Spreer. These have isomorphism signatures gLMPMQccdeeeffffaaaa9aaaaaaaaaaaa9a and gLwMQQcceeeffeffaaaaaaaaaaLaLaLaLaLa. The central surface in each case is a 2-torus, and all four-dimensional and three-dimensional handlebodies have genus one.

Since the fundamental group $\pi_1(S^1 \times S^3) \cong \mathbb{Z}$ and the fundamental group of the central surface surjects onto the fundamental group of each handlebody (as shown in the proof of proposition 5 in ref. 13), it follows that the central surface of any trisection of $S^1 \times S^3$ has genus of at least one. Hence, we recover the result of ref. 14 in *Corollary 10*.

Corollary 10. *The trisection genus of $S^1 \times S^3$ is one.*

We note that $S^1 \times S^3$ also has a triangulation with just two pentachora, cMkabbb2aHaua2a, and therefore, application of *Corollary 6* merely gives a bound of $g(\Sigma) \leq 120$. This highlights the fact that, while our main bound gives a linear upper bound on the minimal genus of a central surface, in practice, this may be far from optimal.

Question 11. *Are there interesting families of 4-manifolds for which there exists an algorithm to compute a trisection of minimal genus for each member of the family?*

Question 12. *Are there interesting families of 4-manifolds for which one can find ts-tricolorable triangulations in which the central surface is of minimal genus?*

Our current techniques allow us to first determine a ts-tricolored triangulation with a large number of pentachora and then collapse this to a smaller triangulation. This could be improved with better heuristics to produce tricolorable triangulations to which we apply 2–4 moves to obtain a ts-tricolored triangulation.

An indispensable tool for experimentation is an implementation of our algorithms and heuristic procedures in Regina. This has recently been carried out and extended using algorithmic tools from discrete Morse theory by Spreer and Tillmann (21). Experimental data for the Budney–Burton census and links to code can be found in ref. 21. As a consequence, the two questions above were recently answered affirmatively for the family of all standard simply connected PL 4-manifolds in ref. 21.

ACKNOWLEDGMENTS. We thank the American Institute for Mathematics and the organizers of the workshop Trisections and Low-Dimensional Topology, where this work was initiated, and thank Jeff Meier and Jonathan Spreer for helpful discussions. We also thank the anonymous referee for helpful comments. J.H. was partially supported by National Science Foundation Grant DMS-1719582-0. The research of J.H.R. and S.T. is partially supported by Australian Research Council Discovery Funding Scheme Project DP160104502. S.T. thanks the Deutsche Forschungsgemeinschaft Collaborative Center Transregionaler Sonderforschungsbereich 109 at Technische Universität Berlin, where parts of this work have been carried out, for its hospitality.

1. Thompson A (1994) Thin position and the recognition problem for S^3. *Math Res Lett* 1:613–630.
2. Jaco W, Rubinstein JH (2003) 0-efficient triangulations of 3-manifolds. *J Differ Geom* 65:61–168.
3. Frigerio R, Petronio C (2004) Construction and recognition of hyperbolic 3-manifolds with geodesic boundary. *Trans Amer Math Soc* 356:3243–3282.
4. Dunfield NM, Hirani AN (2011) The least spanning area of a knot and the optimal bounding chain problem. *Computational Geometry (SCG'11)*, eds Hurtado F, van Kreveld M (ACM, New York), pp 135–144.
5. Li T (2011) An algorithm to determine the Heegaard genus of a 3-manifold. *Geom Topol* 15:1029–1106.
6. Schleimer S (2011) Sphere recognition lies in NP in Low-dimensional and symplectic topology. *Proceedings of Symposia in Pure Mathematics*, ed Usher M (American Math Society, Providence, RI), Vol 82, pp 183–213.
7. Coward A, Lackenby M (2014) An upper bound on Reidemeister moves. *Amer J Math* 136:1023–1066.
8. Hoffman N, et al. (2016) Verified computations for hyperbolic 3-manifolds. *Exp Math* 25:66–78.
9. Burton BA, Downey RG (2017) Courcelle's theorem for triangulations. *J Combin Theor Ser A* 146:264–294.
10. Budney R, Burton BA, Hillman J (2012) Triangulating a Cappell-Shaneson knot complement. *Math Res Lett* 19:1117–1126.
11. Casali MR, Cristofori P, Gagliardi C (2016) Classifying PL 4-manifolds via crystallizations: Results and open problems. *A Mathematical Tribute to Professor José María Montesinos Amilibia*, eds Castrillon M, Martın-Peinador E, Rodrıguez-Sanjurjo JM, Ruiz JM (Departamento de Geometrıa y Topologıa, Facultad de Ciencias Matematicas – Universidad Complutense de Madrid, Madrid), pp 199–226.
12. Rubinstein JH, Tillmann S (2015) Even triangulations of *n*-dimensional pseudo-manifolds. *Algebr Geom Topol* 15:2949–2984.
13. Rubinstein JH, Tillmann S (2016) Multisections of piecewise linear manifolds. *Indiana Univ Math J*, in press.
14. Gay D, Kirby R (2016) Trisecting 4-manifolds. *Geom Topol* 20:3097–3132.
15. Cairns SS (1944) Introduction of a Riemannian geometry on a triangulable 4-manifold. *Ann Math* 45:218–219.
16. Cairns SS (1961) The manifold smoothing problem. *Bull Amer Math Soc* 67:237–238.
17. Whitehead JHC (1940) On C^1-complexes. *Ann Math* 41:809–824.
18. Seifert H, Threlfall W (1980) *A Textbook of Topology*, trans Goldman MA (Academic, New York), Vol 89.
19. Lacher RC (1977) Cell-like mappings and their generalizations. *Bull Amer Math Soc* 83:495–552.
20. Burton BA (2011) The Pachner graph and the simplification of 3-sphere triangulations. *Computational Geometry (SCG'11)*, eds Hurtado F, van Kreveld M (ACM, New York), pp 153–162.
21. Spreer J, Tillmann S (2018) The trisection genus of the standard simply connected PL 4-manifolds. *Proceedings of the 34th International Symposium on Computational Geometry (SoCG 2018), Leibniz International Proceedings in Informatics*, eds Speckmann B, Tóth CD (Schloss Dagstuhl–Leibniz-Zentrum fuer Informatik, Dagstuhl, Germany), Vol 99, pp 71:1–71:13.